

## Experimental research of high field pinning centers in 2% C doped MgB<sub>2</sub> wires at 20 K and 25 K

D. Gajda, A. Morawski, A. J. Zaleski, W. Häßler, K. Nenkov, M. Małeczka, M. A. Rindfleisch, M. S. A. Hossain, and M. Tomsic

Citation: [Journal of Applied Physics](#) **120**, 113901 (2016); doi: 10.1063/1.4962399

View online: <https://doi.org/10.1063/1.4962399>

View Table of Contents: <http://aip.scitation.org/toc/jap/120/11>

Published by the [American Institute of Physics](#)

---

### Articles you may be interested in

[The critical parameters in in-situ MgB<sub>2</sub> wires and tapes with ex-situ MgB<sub>2</sub> barrier after hot isostatic pressure, cold drawing, cold rolling and doping](#)

[Journal of Applied Physics](#) **117**, 173908 (2015); 10.1063/1.4919364

[Enhanced higher temperature \(20–30 K\) transport properties and irreversibility field in nano-Dy<sub>2</sub>O<sub>3</sub> doped advanced internal Mg infiltration processed MgB<sub>2</sub> composites](#)

[Applied Physics Letters](#) **105**, 112603 (2014); 10.1063/1.4896259

[Enhancement of the critical current density and flux pinning of MgB<sub>2</sub> superconductor by nanoparticle SiC doping](#)

[Applied Physics Letters](#) **81**, 3419 (2002); 10.1063/1.1517398

[Al-doped MgB<sub>2</sub> materials studied using electron paramagnetic resonance and Raman spectroscopy](#)

[Applied Physics Letters](#) **108**, 202601 (2016); 10.1063/1.4949338

[High critical current density of MgB<sub>2</sub> bulk superconductor doped with Ti and sintered at ambient pressure](#)

[Applied Physics Letters](#) **79**, 1154 (2001); 10.1063/1.1396629

[Homogeneous carbon doping of magnesium diboride by high-temperature, high-pressure synthesis](#)

[Applied Physics Letters](#) **104**, 162603 (2014); 10.1063/1.4871578

---

**AIP** | Journal of  
Applied Physics

SPECIAL TOPICS



## Experimental research of high field pinning centers in 2% C doped MgB<sub>2</sub> wires at 20 K and 25 K

D. Gajda,<sup>1,2,a)</sup> A. Morawski,<sup>3</sup> A. J. Zaleski,<sup>4,2</sup> W. Häbler,<sup>5</sup> K. Nenkov,<sup>1,5</sup> M. Mafecka,<sup>4</sup> M. A. Rindfleisch,<sup>6</sup> M. S. A. Hossain,<sup>7</sup> and M. Tomsic<sup>6</sup>

<sup>1</sup>International Laboratory of High Magnetic Fields and Low Temperatures (HMF and LT), Gajowicka 95, 53-421 Wrocław, Poland

<sup>2</sup>Centre for Advanced Materials and Smart Structures, Polish Academy of Sciences, Okólna 2, 50-950 Wrocław, Poland

<sup>3</sup>Institute of High Pressure Physics, Polish Academy of Sciences (PAS), Sokołowska 29/37, 01-142 Warsaw, Poland

<sup>4</sup>Institute of Low Temperature and Structure Research, PAS, Okólna 2, 50-422 Wrocław, Poland

<sup>5</sup>Institute for Solid State and Materials Research Dresden, P.O. Box 270016, D-01171 Dresden, Germany

<sup>6</sup>Hyper Tech Research, Inc., 539 Industrial Mile Rd, Columbus, Ohio 43228, USA

<sup>7</sup>Institute for Superconducting and Electronic Materials, Australian Institute of Innovative Materials (AIIM), University of Wollongong, North Wollongong, New South Wales 2519, Australia

(Received 21 July 2016; accepted 26 August 2016; published online 15 September 2016)

High field pinning centers in MgB<sub>2</sub> doped with 2 at. % carbon under a low and a high hot isostatic pressures have been investigated by transport measurements. The field dependence of the transport critical current density was analyzed within the different pinning mechanisms: surface pinning, point pinning, and pinning due to spatial variation in the Ginzburg-Landau parameter ( $\Delta\kappa$  pinning). Research indicates that a pressure of 1 GPa allows similar pinning centers to  $\Delta\kappa$  pinning centers to be obtained. This pinning is very important, because it makes it possible to increase the critical current density in high magnetic fields at 20 K and 25 K. Our results indicate that the  $\delta T_c$  and  $\delta l$  pinning mechanisms, which are due to a spatial variation in the critical temperature ( $T_c$ ) and the mean free path,  $l$ , respectively, create dislocations. The high density of dislocations with inhomogeneous distribution in the structure of the superconducting material creates the  $\delta l$  pinning mechanism. The low density of dislocations with inhomogeneous distribution creates the  $\delta T_c$  pinning mechanism. Research indicates that the hot isostatic pressure process makes it possible to obtain a high dislocation density with a homogeneous distribution. This allows us to obtain the  $\delta T_c$  pinning mechanism in MgB<sub>2</sub> wires. In addition, a high pressure increases the crossover field from the single vortex to the small vortex bundle regime ( $B_{sb}$ ) and improves the  $\delta T_c$  pinning mechanism. Our research has proved that a high pressure significantly increases the crossover field from the small bundle to the thermal regime ( $B_{th}$ ), with only a modest decrease in  $T_c$  of 1.5 K, decreases the thermal fluctuations, increases the irreversibility magnetic field ( $B_{irr}$ ) and the upper critical field ( $B_{c2}$ ) in the temperature range from 4.2 K to 25 K, and reduces  $B_{irr}$  and  $B_{c2}$  above 25 K. Published by AIP Publishing. [<http://dx.doi.org/10.1063/1.4962399>]

### I. INTRODUCTION

In a superconducting material in the mixed state, vortices appear. The Lorentz force causes motion of these vortices, which, in turn, reduce the critical current density ( $J_c$ ). These vortices can be anchored by using pinning centers, leading to an increase in  $J_c$ . The pinning centers create normal conducting areas, weak superconducting areas, and inclusions. Livingston<sup>1</sup> and Wang *et al.*<sup>2</sup> identified four types of pinning centers: volume pinning centers (e.g., big voids), surface pinning centers (grain boundaries), point pinning centers (e.g., precipitates with sizes near the coherence length), and line pinning centers (dislocations). The critical current density in the superconducting ceramic materials also depends on the connections between the grains.

Currently, we have several models for analyzing the dominant pinning mechanism, e.g., Dew-Hughes,<sup>3</sup> identification of the  $\delta T_c$  and  $\delta l$  pinning mechanisms,<sup>4</sup> and Higuchi *et al.*<sup>5</sup> Dew-Hughes proposed several formulas for various pinning mechanisms, e.g., point ( $h(1-h)^2$ —e.g., precipitates and voids of about the coherence length in size and dislocations), surface ( $h^{0.5}(1-h)^2$ —grain boundaries), and volume ( $h^0(1-h)^2$ —large voids and precipitates), where  $h$  is the magnetic field normalized by the irreversibility field ( $B_{irr}$ ). Research indicates that the dislocations create high field pinning centers, because they increase the critical current density in high magnetic fields.<sup>6,7</sup> Currently, we have two types of edge and screw dislocations. Dam *et al.* proposed that both types of dislocations anchor vortices in the same way.<sup>8</sup> The results reported in the literature indicate that the surface and volume pinning increase the critical current density ( $J_c$ ) in low magnetic fields, while the point pinning centers increase  $J_c$  in the middle and high magnetic fields.<sup>9</sup>

<sup>a)</sup>Author to whom correspondence should be addressed. Electronic mail: dangajda@op.pl

The  $\delta l$  pinning mechanism is associated with charge carrier mean free path variations, and the  $\delta T_c$  pinning mechanism is linked to randomly distributed spatial variations in the transition temperature.<sup>9</sup> Magnetic measurements reported by Motaman *et al.*<sup>10</sup> and Ghorbani *et al.*<sup>9,11</sup> indicate that the  $\delta l$  pinning mechanism is dominant at low temperature, and the  $\delta T_c$  pinning mechanism is dominant at high temperature. In addition, studies indicate that an undoped MgB<sub>2</sub> material has  $\delta T_c$  as its dominant pinning mechanism and that a doped MgB<sub>2</sub> material has  $\delta l$  as its dominant pinning mechanism.<sup>2,12</sup> The effectiveness of these pinning centers is the greatest for a high Ginzburg-Landau ( $\kappa$ ) parameter. Higuchi *et al.* proposed three types of pinning mechanisms, e.g., surface pinning, point pinning, and  $\Delta\kappa$  pinning.<sup>5,13</sup> The results in the literature suggest that the surface pinning centers increase the critical current density in the low magnetic fields. On the other hand, the point pinning centers and the  $\Delta\kappa$  pinning increase  $J_c$  in the middle and high magnetic fields.

High field pinning centers (dislocations) can be created by two methods: cold treatment and hot treatment. The different types of cold treatment include cold isostatic pressure (CIP<sup>14</sup>), cold drawing,<sup>1</sup> and equal channel multi-angle pressing (ECMAP<sup>15</sup>). These dislocations vanish as a result of thermal processes, however. The sintering for synthesizing an *in situ* MgB<sub>2</sub> material also creates dislocations, e.g., the substitution of C on B sites in MgB<sub>2</sub><sup>16</sup> and the shrinkage of the MgB<sub>2</sub> material.<sup>17</sup> These processes create an inhomogeneous distribution of dislocations. Only a hot isostatic pressure (HIP) makes it possible to obtain a homogeneous distribution of dislocations.<sup>18,19</sup> A homogeneous distribution of dislocations is very important, because it allows us to obtain a homogeneous distribution of the high field pinning centers. This leads to a high critical current density in the high magnetic fields.

Previous studies of the  $\delta T_c$  and  $\delta l$  pinning mechanisms were performed by using magnetic measurements.<sup>2,4,9-12</sup> We will show results on the  $\delta T_c$  and  $\delta l$  pinning mechanisms that were obtained by the transport measurements. In addition, in this article, we analyze the pinning mechanisms using the methods of Dew-Hughes and Higuchi *et al.* We also show the effects of high pressure on the structure of the MgB<sub>2</sub> material, as well as  $T_c$ ,  $B_{irr}$ , the upper critical field ( $B_{c2}$ ), and  $J_c$ . Moreover, we will show that the distribution of pinning centers can have a decisive influence on the  $J_c$  at 20 K and 25 K. We will show that dislocations create high field pinning centers. These pinning centers also increase  $J_c$  at a high temperature.

## II. PREPARATION OF SAMPLES

The wires were made at Hyper Tech Research using a continuous tube forming and filling (CTFF) process.<sup>20</sup> The MgB<sub>2</sub> wires had 36 filaments and a Nb barrier. The filaments comprised a nano-sized B, pre-doped with 2 at. % C with an Mg to B ratio of 1:2. The wires were fabricated to a diameter of 0.83 mm, achieving a fill factor of 14%. All the wires were annealed under an isostatic pressure at the Institute of High Pressure Research in Warsaw.<sup>21</sup> The HIP was a two-step process: the isostatic pressure was first applied, and then

the wire sample was ramped to the set annealing temperature. The HIP process was ended by decreasing the annealing temperature to room temperature before decreasing the isostatic pressure. The samples were annealed at 700 °C at pressures between 0.1 MPa and 1 GPa (Table I). The HIP was performed in a 5 N argon atmosphere in a high gas pressure chamber. The transport critical current ( $I_c$ ) of the MgB<sub>2</sub> wires was measured by the four-probe resistive method at 10 K, 20 K, and 25 K at the Institute for Solid State and Materials Research Dresden.<sup>22</sup> The  $I_c$  was determined on the basis of the 1  $\mu$ V/cm criterion. The critical temperature and the critical magnetic fields were measured using the four-probe resistive method on a physical properties measurement system (PPMS), operating at 100 mA and 15 Hz at the International Laboratory of HMF and LT.<sup>23,24</sup>  $T_c$ ,  $B_{irr}$ , and  $B_{c2}$  were determined with the respective criteria of 50%, 10%, and 90% of the normal state resistance. An analysis of the microstructure was performed using a scanning electron microscope (SEM; FEI Nova Nano SEM 230) at the Institute of Structural Research and Low Temperatures in Wroclaw, PAS.

## III. RESULTS

Fig. 1(a) shows the results of scanning electron microscopy (SEM) for sample A (HIP at 0.1 MPa). These results indicate that annealing under a low pressure creates large voids, large grains, lower MgB<sub>2</sub> material density, and an inhomogeneous distribution of voids and grains. In addition, a low pressure (with the high pressure) reduces the number of connections between the grains and creates an inhomogeneous distribution of connections between the grains (with greater and fewer number of connections at different locations). This leads to an inhomogeneous distribution of the pinning centers and may facilitate the movement of the dislocations. On the other hand, results from sample C indicate that annealing under a high pressure creates small voids, small grains, and a better MgB<sub>2</sub> material density, producing a homogeneous distribution of grains (Fig. 1(b)). In addition, a high pressure increases the number of connections between the grains and creates a homogeneous distribution of connections between the grains. This leads to a homogeneous distribution of the pinning centers and a better distribution of the dislocations.

The results in Fig. 2 show that a pressure of 1 GPa decreases the  $T_c$  by 1.5 K in  $B=0$  T (sample A: 34 K and sample C: 32.5 K). A longer annealing time (90 min) does not change the  $T_c$  ( $B=0$  T). In addition, our studies indicate

TABLE I. The parameters of the HIP process for the samples in this study.

Sample identifier	HIP annealing time (min)	temperature (°C)	pressure (Pa)
A	15	700	0.1 M
B	15	700	0.4 G
C	15	700	1 G
D	60	700	1 G
E	90	700	1 G

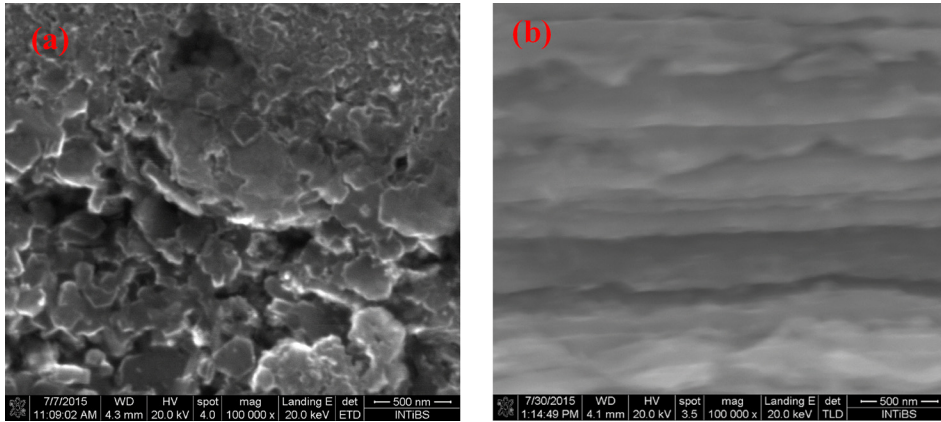


FIG. 1. The SEM images of a longitudinal section of C doped  $\text{MgB}_2$  wire with a monel sheath and a Nb barrier: (a) Sample A: after the HIP process at 0.1 MPa and 700 °C for 15 min and (b) sample C: after HIP at 1 GPa and 700 °C for 15 min.

that a high pressure increases the  $T_c$  above 8 T,  $B_{\text{irr}}$ , and  $B_{c2}$  below 16 K, does not change the  $T_c$  in the range from 4 T to 8 T,  $B_{\text{irr}}$ , or  $B_{c2}$  in the range from 16 K to 25 K, and decreases the  $T_c$  below 4 T,  $B_{\text{irr}}$ , and  $B_{c2}$  above 25 K. These results are very important, because they indicate the temperature range in which the HIP process increases the critical parameters. The results presented by Monteverde *et al.*,<sup>25</sup> Lorenz *et al.*,<sup>26</sup> and Bordet *et al.*<sup>27</sup> indicated that decrease of the  $T_c$  might result from an increasing phonon frequency with an increased pressure, which broadens the density of state and lowers it on the Fermi surface. The reduction of the  $T_c$  of a wire under pressure during reaction would then be related to the loss of  $p_{xy}$  holes, the reduction of lattice parameters, and the reduction of  $c/a$  ratio (this effect can create a dislocation).<sup>25–27</sup> Serquis *et al.*,<sup>18</sup> however, have proposed that the HIP process creates strains, and this is the mechanism by which it reduces the  $T_c$ .<sup>28</sup>  $\text{MgB}_2$  experiences a large

shrinkage during the synthesis reactions at temperatures above 650 °C. The shrinking creates stress (dislocations). Buzea and Yamashita<sup>29</sup> proposed that the shrinkage of the  $\text{MgB}_2$  crystal unit cell reduces the  $T_c$  by 1 K. Studies presented by Ghorbani *et al.*,<sup>13</sup> Kazakov *et al.*,<sup>16</sup> and Mudgel *et al.*<sup>30</sup> indicate that the C substitution on the B sites in the lattice creates a lattice distortion (strain) and disorder in the sigma band. It also leads to a reduction in the  $T_c$ . Our study on the undoped  $\text{MgB}_2$  wires showed that 1 GPa pressure decreases the  $T_c$  by 1.5 K, increases the critical parameters in the range of 10 K to 27 K, and decreases the critical parameters above 27 K.<sup>19</sup> The similar influence of the isostatic pressure to that of C doping on the  $T_c$  may indicate that the isostatic pressure creates a lattice distortion. This is confirmed by the study of Serquis *et al.*<sup>18</sup> We believe that this effect decreases the  $T_c$  and the critical parameters above 25 K and increases the critical parameters below 16 K. Based

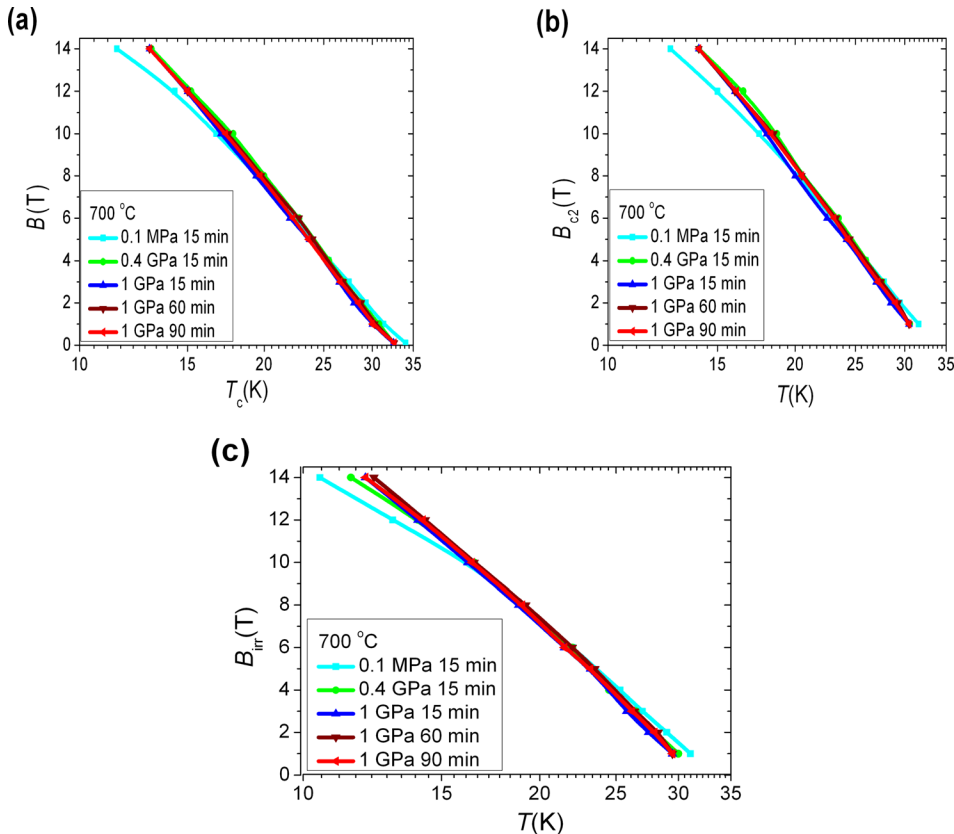


FIG. 2. The transport measurements for C doped  $\text{MgB}_2$  wires after annealing in pressures from 0.1 MPa to 1 GPa: (a) the magnetic field dependence on the critical temperature ( $T_c$ ); (b) upper critical fields ( $B_{c2}$ ) dependence on the temperature; and (c) irreversibility magnetic field ( $B_{\text{irr}}$ ) dependence on the temperature.

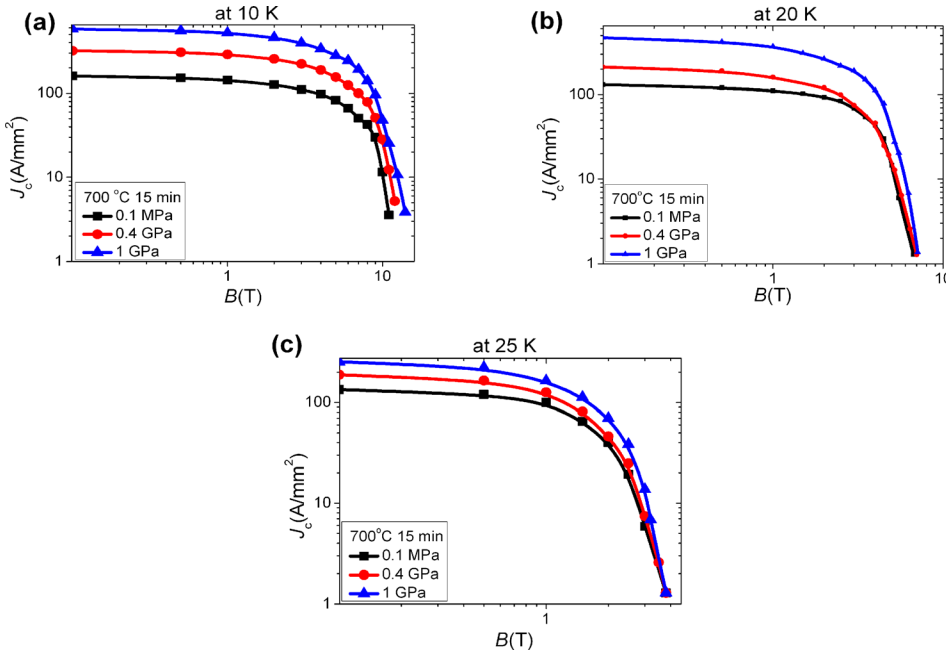


FIG. 3. Critical current density dependence on the magnetic field for samples A–C: (a) at 10 K, (b) at 20 K, and (c) at 25 K.

on the results in Fig. 2 and the results for the undoped  $\text{MgB}_2$  wires,<sup>19</sup> we can deduce that a higher level of C doping and a higher pressure will cause a further reduction of critical parameters at higher temperatures (20 K–39 K). This indicates that a pressure of 1 GPa and a small amount of dopant are the optimum conditions. The shrinkage of the  $\text{MgB}_2$  material during the solid-state reaction between Mg and B is small, about 5%, indicating that this effect does not significantly influence the  $T_c$ .<sup>31</sup> Monteverde *et al.*<sup>25</sup> proposed that the pressure decreases resistance in the normal state. The results in Fig. 1 suggest that this reduction may produce a greater number of connections between the grains.

The results in Fig. 3 show that a pressure of 0.4 GPa increases  $J_c$ , e.g., at 10 K by about 200%, at 20 K by about 10%–30% (in magnetic fields from 0 T to 2 T), and at 25 K by 15%–25% (in magnetic fields from 0 T to 1 T). Further increasing the pressure to about 0.6 GPa also increases  $J_c$ , e.g., at 10 K by about 100%, at 20 K by about 200%, and at 25 K by about 30% to 60%. An analysis of Fig. 4 allows us to determine the crossover fields from the single vortex to the small vortex bundle regime ( $B_{sb}$ ) and from the small bundle regime to the thermal fluctuations regime ( $B_{th}$ ).<sup>9</sup> Based on the transport measurements (Figs. 2 and 4), we have developed the  $B$  -  $T$  phase diagram in Fig. 5. In this diagram, the region below  $B_{sb}$  is associated with single vortex pinning, the region between  $B_{sb}$  and  $B_{th}$  small bundle pinning, the region between  $B_{th}$  and  $B_{irr}$  thermal fluctuations, the region between  $B_{irr}$  and  $B_{c2}$  vortex liquid, and the region above  $B_{c2}$  the normal state. The results in Fig. 5 for  $B_{th}$  show that a high pressure significantly reduces the thermal fluctuations and increases the region of small bundle pinning (the first such result). This result is very important, because it indicates the reason for a low  $J_c$  in the  $\text{MgB}_2$  wires annealed at a low pressure (0.1 MPa). It is important that the HIP process can significantly reduce the thermal fluctuations above 20 K. A reduction of thermal fluctuations can cause a greater amount and a more homogeneous distribution of small

bundle pinning, eliminate pure Mg (since pure magnesium has low resistivity), and lead to a greater number of connections between the grains. Our result also shows that a pressure of 1 GPa increases  $B_{sb}$ . We believe that a higher crossover field  $B_{sb}$  might indicate a greater amount of pinning centers that are more homogeneously distributed. The shape of the  $B_{sb}$  curves in Fig. 5 is similar to the curve of the  $\delta T_c$  pinning mechanism.<sup>4</sup> This indicates that a high pressure does not change the pinning mechanism.

We analyzed the pinning mechanism by using the Dew-Hughes' model, e.g., point pinning:  $f(h_1) = A(h_1)^1(1 - h_1)^2$  and surface pinning:  $f(h_1) = A(h_1)^{0.5}(1 - h_1)^2$ , where  $A$  is a parameter and  $h_1 = B/B_{irr}$ . The results in Fig. 6(a) show that in the range from  $h_1 = 0$  to 0.6, the point pinning mechanism is dominant, and, from 0.7 to 1, the surface pinning mechanism is dominant. This suggests that the samples have an insufficient number of high field pinning centers. Similar scaling results were obtained at 10 K and 25 K. We see that a

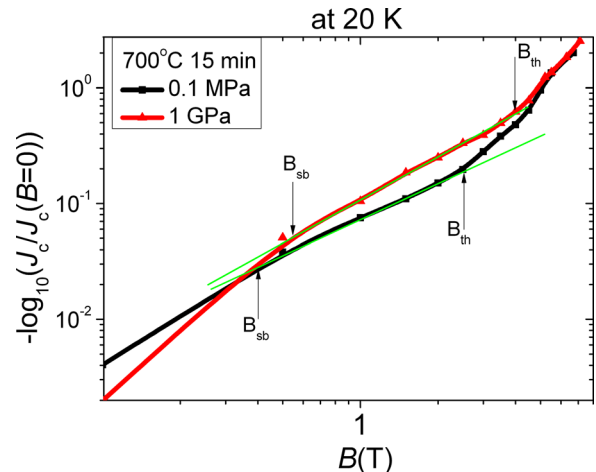


FIG. 4. A double logarithmic plot of  $-\log[J_c(B)/J_c(0)]$  as a function of  $B$  at 20 K for samples A (0.1 MPa) and C (1 GPa). The crossover fields  $B_{sb}$  and  $B_{th}$  are marked by arrows.

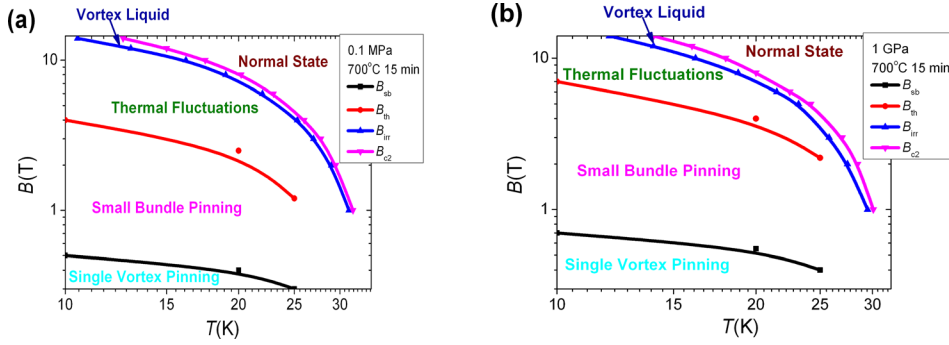


FIG. 5. A phase diagram for 2 at. % C doped  $\text{MgB}_2$  wires.  $B_{sb}$  and  $B_{th}$  were obtained from the transport measurement data on  $J_c(B)$  (see Fig. 3).  $B_{irr}(T)$  and  $B_{c2}(T)$  were obtained from the transport measurement data (see Fig. 2): (a) sample A and (b) sample C.

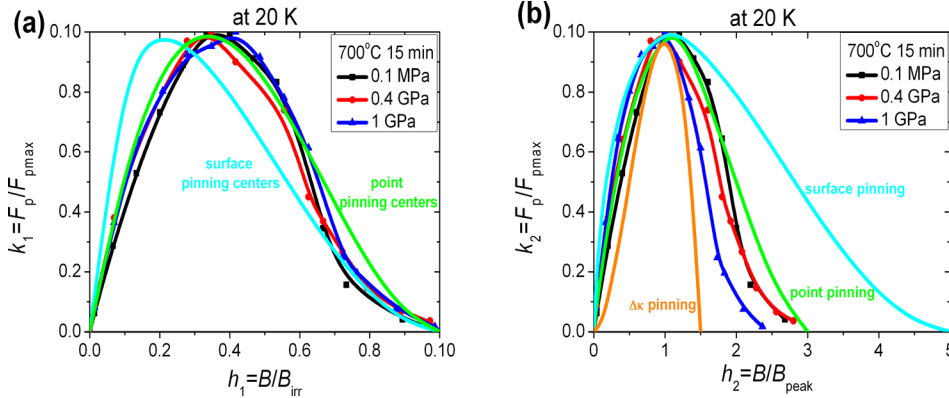


FIG. 6. (a) The reduced pinning force depending on the reduced magnetic field  $B/B_{irr}$  for samples A–C—an analysis of pinning by the Dew-Hughes' model<sup>7</sup> at 20 K, and (b) the reduced pinning force depending on the reduced magnetic field  $B/B_{peak}$  for samples A–C—an analysis of pinning by the model of Higuchi *et al.*<sup>9</sup> at 20 K.

high pressure does not change the dominant pinning mechanism. This indicates that the high pressure increases the amount of pinning centers and the number of connections between the grains (Fig. 1). This leads to an increased  $J_c$ .

We also analyzed the pinning mechanism by using the method of Higuchi *et al.*:<sup>5</sup>  $f(h_2) = (9/4)h_2(1 - h_2/3)^2$  for normal point pinning,  $f(h_2) = (25/16)(h_2)^{0.5}(1 - h_2/5)^2$  for surface pinning, and  $f(h_2) = (3h_2)^2(1 - 2h_2/3)$  for  $\Delta\kappa$  pinning, where  $h_2 = B/B_{peak}$ . Fig. 6(b) shows that the low pressure (0.1 MPa) leads to the normal point pinning in the range from 0 to 2 T. The 0.4 GPa pressure slightly shifts the curve of sample B from normal point pinning to  $\Delta\kappa$  pinning in the range from 1 to 2 T. A high pressure of 1 GPa shifts the pinning mechanism to  $\Delta\kappa$  pinning. This indicates that the high pressure creates the dislocations (high field pinning centers).

The results in Fig. 7 show that a high pressure increases the  $J_c$  at high temperature (10 K–26 K) in 2 T. A long annealing time slightly increases  $J_c$ . Moreover, the shape of the curves in Fig. 7 is similar to the curve for the  $\delta T_c$  pinning mechanism.<sup>2</sup> This may indicate that a high pressure does not adversely affect the  $\delta T_c$  pinning mechanism.

The results in Fig. 8 show that a longer annealing time increases the  $J_c$  modestly at lower temperatures but more markedly at higher temperatures: at 10 K, by about 15%–70%; at 20 K, by about 30%–90%; and at 25 K, by 100%. Moreover, a long annealing does not increase  $B_{sb}$  or  $B_{th}$  (Fig. 9) and does not change the dominant pinning mechanism in the range from 10 K to 25 K (Fig. 10). No change in the dominant pinning mechanism indicates that an annealing over a longer time creates more connections between the grains and increases the pinning center density. These factors increase  $J_c$  at a temperature range from 10 K to 25 K.

#### IV. DISCUSSION

Previous reports on the  $\delta T_c$  and the mean free path  $\delta l$  pinning mechanisms were based on the magnetic results (magnetic critical current density,  $J_{cm}$ ).<sup>2,4,9–12</sup> The research presented by Shi indicated that the transport current flows mainly through the longitudinal connections.<sup>32</sup> In contrast, the magnetic current flows in the grains and transverse connections.<sup>32</sup> In our paper, we present the transport measurement results, which relate to the longitudinal connections. On the basis of the three pinning mechanisms, we will examine the impact of additives and a high isostatic pressure for the creation of the pinning centers.

Studies show that doping with C makes the  $\delta l$  pinning mechanism dominant.<sup>2,10,33</sup> The authors of these studies

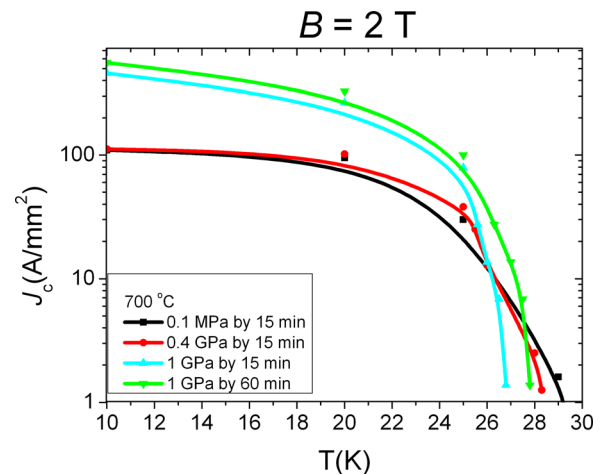


FIG. 7. The critical current density dependence on the temperature in  $B = 2$  T for samples A–D.

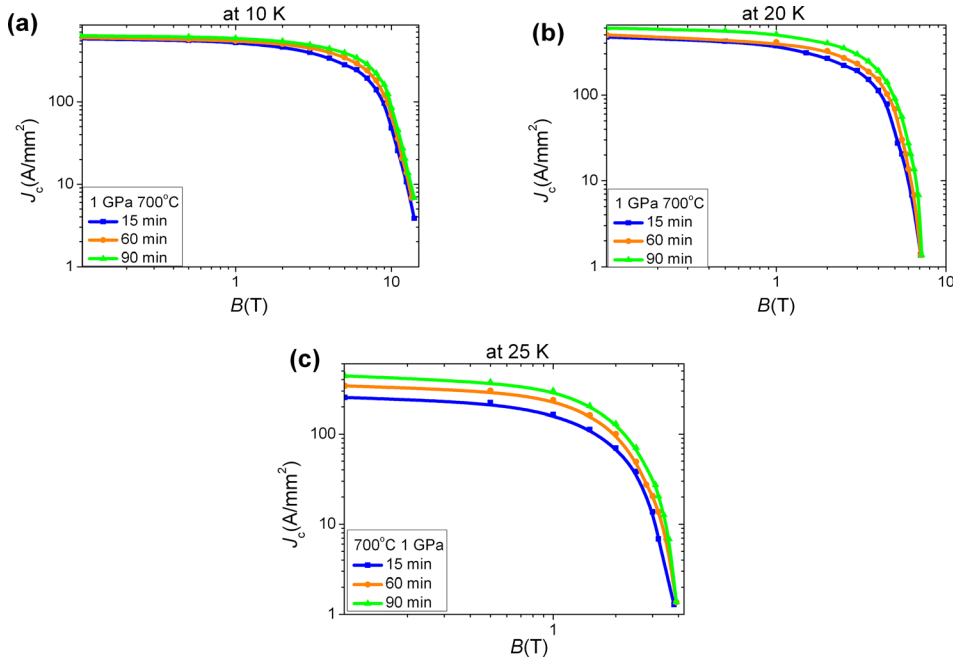


FIG. 8. The critical current density dependence on the magnetic field for samples C–E (a) at 10 K, (b) at 20 K, and (c) at 25 K.

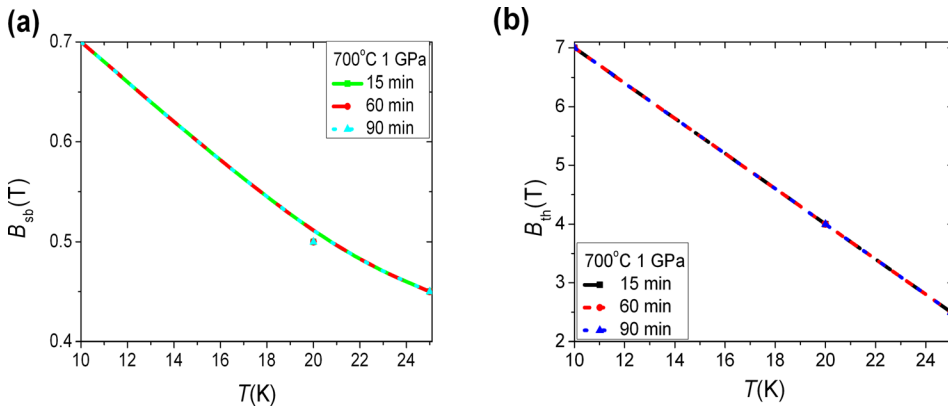


FIG. 9. (a) The crossover fields  $B_{sb}$  for samples C–E depending on the temperature and (b) the crossover fields  $B_{th}$  for samples C–E depending on temperature.

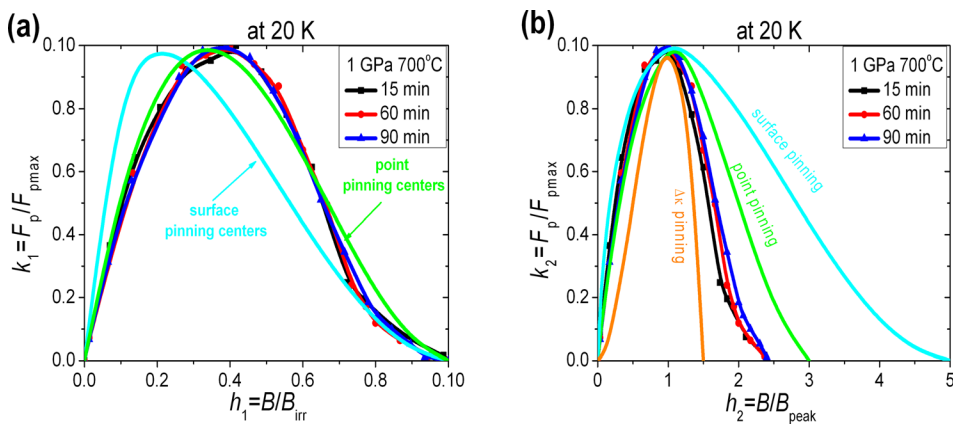


FIG. 10. (a) The reduced pinning force depending on the reduced magnetic fields  $B/B_{irr}$  for samples C–E—an analysis pinning of Dew-Hughes' model<sup>7</sup> at 20 K and (b) the reduced pinning force depending on the reduced magnetic fields  $B/B_{peak}$  for samples C, D, and E—an analysis of pinning by the model of Higuchi *et al.*<sup>9</sup> at 20 K.

have shown that C is substituted for B, creating the dislocations. This indicates that the dislocations create the  $\delta I$  pinning mechanism. In addition, the dopant is non-uniformly distributed in the structure of the superconducting material, leading to a non-uniform distribution of dislocations in the superconducting material. These authors showed that undoped  $MgB_2$  material features the  $\delta T_c$  pinning mechanism (for annealing above 650 °C).<sup>2,11,12,33</sup> A heat treatment of the  $MgB_2$

material above 650 °C (the melting point of Mg), however, causes a strong shrinkage of the  $MgB_2$  material, even by 25%.<sup>17</sup> The shrinkage of the material leads to the creation of dislocations. This indicates that dislocations also create the  $\delta T_c$  pinning mechanism. The dislocation density created by the shrinkage is smaller, however (small reduction of  $T_c$  of about 1 K (Ref. 29)). A high dislocation density with an inhomogeneous distribution causes large fluctuations in the

mean free path. This factor at higher temperature (20 K) significantly decreases  $T_c$ ,  $B_{irr}$ ,  $B_{c2}$ , and  $J_c$ . A smaller dislocation density with an inhomogeneous distribution causes smaller fluctuations in the mean free path. This leads to a smaller reduction in the critical parameters at high temperatures (above 20 K) and would explain why the small amount of doping (at 2% C) in our wires does not create the  $\delta l$  pinning mechanism. Studies indicate that the HIP process increases the dislocation density in the MgB<sub>2</sub> material. This should create the  $\delta l$  pinning mechanism. Our research indicates, however, that we obtain the  $\delta T_c$  pinning mechanism. This may be because the HIP process creates a uniform distribution of dislocations in the superconducting material. A high dislocation density with a homogeneous distribution causes smaller fluctuations in the mean free path. This leads to the  $\delta T_c$  pinning mechanism and increases the critical parameters at high temperature.

The results presented by Embon suggest that a vortex typically interacts with small clusters of a few pinning defects separated by about the coherence length.<sup>34</sup> This may mean that the random distribution of pinning centers causes a strong clustering of the vortices. This leads to a reduction in the critical parameters. In contrast, a homogeneous distribution of the pinning centers reduces the clustering of pinning centers and thus of vortices, leading to an increase in the critical parameters. Moreover, the results in Ref. 34 indicate that a random configuration of the pinning centers (defects) leads to a greater thermally activated depinning of vortices, even in the case of strong pinning. Our research shows that the HIP process significantly reduces the thermal fluctuations. This might indicate that the HIP process leads to a more uniform distribution of the pinning centers.

The  $\delta T_c$  and  $\delta l$  pinning mechanisms have mainly been associated with the effects of the temperature on pinning centers. In contrast, the models of Dew-Hughes<sup>3</sup> and Higuchi *et al.*<sup>5</sup> mainly deal with the effects of the magnetic field on the pinning centers. Our results suggest that both the methods lead to similar results. The Dew-Hughes' method in Fig. 6(a) shows that we do not have pinning points above  $h_1 = 0.6$  (high field pinning centers), although this method does not indicate which type of defect is missing (precipitates with a thickness similar to the coherence length or dislocations). The Higuchi model shows that we do not have enough strong high field pinning centers. This analysis strongly suggests that we have a small amount of  $\Delta\kappa$  pinning centers. Our research shows, however, that a high isostatic pressure is a method that can yield a dominant  $\Delta\kappa$  pinning mechanism. The results presented by Livingston indicate that the dislocations mainly create  $\Delta\kappa$  pinning.<sup>1</sup> This suggests that the HIP process increases the dislocation density. The results in Fig. 6(b) indicate that a higher dislocation density reduces the thermal fluctuations and increases  $B_{sb}$ ,  $B_{th}$ , and  $J_c$  at 20 K.

## V. CONCLUSIONS

From our research, a high isostatic pressure of 1 GPa creates the pinning centers similar to the  $\Delta\kappa$  pinning centers. An analysis performed by using the three models of pinning

mechanisms indicates that the dislocations create the  $\Delta\kappa$  pinning centers. Our measurements show that a homogeneous distribution of the  $\Delta\kappa$  pinning centers increases the critical current density at 20 K and 25 K, increases the crossover fields  $B_{sb}$  and  $B_{th}$ , as well as  $B_{irr}$  and  $B_{c2}$ , below 25 K, significantly reduces the thermal fluctuations, and improves the  $\delta T_c$  pinning mechanism. This is a very important result, because it shows that the HIP process can control the process for creating the pinning centers. By controlling the value of the pressure, we can control the sizes of grains and inclusions, the dislocation density, and the density and uniformity of the material. The HIP process is a simpler, easier method and can be used on a wider scale to obtain structure texturing of the MgB<sub>2</sub> material than thin film methods. Our results show that the HIP process increases  $J_c$  by about 200%.

<sup>1</sup>J. D. Livingston, see [www.bnl.gov/magnets/staff/gupta/Summer1968/0377.pdf](http://www.bnl.gov/magnets/staff/gupta/Summer1968/0377.pdf) for GE R&D Center Report (1969–1970).

<sup>2</sup>J. L. Wang, R. Zeng, J. H. Kim, L. Lu, and S. X. Dou, *Phys. Rev. B* **77**, 174501 (2008).

<sup>3</sup>D. Dew-Hughes, *Philos. Mag.* **30**, 293 (1974).

<sup>4</sup>M. J. Qin, X. L. Wang, H. K. Liu, and S. X. Dou, *Phys. Rev. B* **65**, 132508 (2002).

<sup>5</sup>T. Higuchi, S. I. Yoo, and M. Murakami, *Phys. Rev. B* **59**, 1514 (1999).

<sup>6</sup>M. Panek, D. Pattanayak, R. Meier-Hirmer, and H. Kupfer, *J. App. Phys.* **54**, 7083 (1983).

<sup>7</sup>Z. Ma, Y. Liu, J. Huo, and Z. Gao, *J. Appl. Phys.* **106**, 113911 (2009).

<sup>8</sup>B. Dam, J. M. Huijbregtse, F. C. Klaassen, R. C. F. van der Geest, G. Doornbos, J. H. Rector, A. M. Testa, S. Freisem, J. C. Martinez, B. Stauble-Pumpin, and R. Griessen, *Nature* **399**, 439 (1999).

<sup>9</sup>S. R. Ghorbani, X. L. Wang, S. X. Dou, S.-I. Lee, and M. S. A. Hossain, *Phys. Rev. B* **78**, 184502 (2008).

<sup>10</sup>A. Motaman, M. S. A. Hossain, X. Xu, K. W. See, K. C. Chung, and S. X. Dou, *Supercond. Sci. Technol.* **26**, 085013 (2013).

<sup>11</sup>S. R. Ghorbani, X. L. Wang, M. S. A. Hossain, S. X. Dou, and S.-I. Lee, *Supercond. Sci. Technol.* **23**, 025019 (2010).

<sup>12</sup>F. X. Xiang, X. L. Wang, X. Xun, K. S. B. De Silva, Y. X. Wang, and S. X. Dou, *Appl. Phys. Lett.* **102**, 152601 (2013).

<sup>13</sup>S. R. Ghorbani, M. Hosseinzadeh, and X. L. Wang, *Supercond. Sci. Technol.* **28**, 125006 (2015).

<sup>14</sup>R. Flukiger, M. S. A. Hossain, and C. Senatore, *Supercond. Sci. Technol.* **22**, 085002 (2009).

<sup>15</sup>V. A. Beloshenko, T. Konstantinova, N. I. Matrosov, V. Z. Spuskanyuk, V. Chishko, D. Gajda, A. J. Zaleski, V. P. Dyakonov, R. Puzniak, and H. Szymczak, *J. Supercond. Novel Mag.* **22**, 505 (2009).

<sup>16</sup>S. M. Kazakov, R. Puzniak, K. Rogacki, A. V. Mironov, N. D. Zhigadlo, J. Jun, Ch. Soltmann, B. Batlogg, and J. Karpinski, *Phys. Rev. B* **71**, 024533 (2005).

<sup>17</sup>A. Jung, S. I. Schlachter, B. Runtsch, B. Ringsdorf, H. Fillinger, H. Orschulko, A. Drechsler, and W. Goldacker, *Supercond. Sci. Technol.* **23**, 095006 (2010).

<sup>18</sup>A. Serquis, L. Civale, D. L. Hammon, X. Z. Liao, J. Y. Coulter, Y. T. Zhu, M. Jaime, D. E. Peterson, F. M. Mueller, V. F. Nesterenko, and Y. Gu, *Appl. Phys. Lett.* **82**, 2847 (2003).

<sup>19</sup>D. Gajda, A. Morawski, A. J. Zaleski, W. Häbeler, K. Nenkov, M. A. Rindfleisch, T. Cetner, and M. Tomsic, *J. Mater. Sci. Eng.* **5**(3), 1000244 (2016).

<sup>20</sup>M. Tomsic, M. Rindfleisch, J. Yue, K. McFadden, J. Phillips, M. D. Sumption, M. Bhatia, S. Bohnenstiehl, and E. W. Collings, *Int. J. Appl. Ceram. Technol.* **4**, 250 (2007).

<sup>21</sup>D. Gajda, A. Morawski, A. Zaleski, T. Cetner, M. Małacka, A. Presz, M. Rindfleisch, M. Tomsic, C. J. Thong, and P. Surdacki, *Supercond. Sci. Technol.* **26**, 115002 (2013).

<sup>22</sup>W. Häbeler, M. Herrmann, C. Rodig, M. Schubert, K. Nenkov, and B. Holzapfel, *Supercond. Sci. Technol.* **21**, 062001 (2008).

<sup>23</sup>D. Gajda, A. Morawski, A. Zaleski, M. Kurnatowska, T. Cetner, G. Gajda, A. Presz, M. Rindfleisch, and M. Tomsic, *Supercond. Sci. Technol.* **28**, 015002 (2015).

<sup>24</sup>D. Gajda, A. Morawski, A. Zaleski, A. Yamamoto, and T. Cetner, *Appl. Phys. Lett.* **108**, 152601 (2016).



- <sup>25</sup>M. Monteverde, M. Nunez-Regueiro, N. Rogado, K. A. Regan, M. A. Hayward, T. He, S. M. Loureiro, and R. J. Cava, *Science* **292**, 75–77 (2001).
- <sup>26</sup>B. Lorenz, R. L. Meng, and C. W. Chu, *Phys. Rev. B* **64**, 12507 (2001).
- <sup>27</sup>P. Bordet, M. Mezouar, M. Nunez-Regueiro, M. Monteverde, M. D. Nunez-Regueiro, N. Rogado, A. Regan, M. A. Hayward, T. He, S. M. Loureiro, and R. J. Cava, *Phys. Rev. B* **64**, 172502 (2001).
- <sup>28</sup>A. Serquis, Y. T. Zhu, E. J. Peterson, J. Y. Coulter, D. E. Peterson, and F. M. Mueller, *Appl. Phys. Lett.* **79**, 4399–4401 (2001).
- <sup>29</sup>C. Buzea and T. Yamashita, *Supercond. Sci. Technol.* **14**, R115–R146 (2001).
- <sup>30</sup>M. Mudgel, L. S. Sharath Chandra, V. Ganesan, G. L. Bhalla, H. Kishan, and V. P. S. Awana, *J. Appl. Phys.* **106**, 033904 (2009).
- <sup>31</sup>M. M. Avedesian and H. Baker, *ASM Specialty Handbook: Magnesium and Magnesium Alloys* (ASM International, Materials Park, OH, 1999).
- <sup>32</sup>Z. X. Shi, M. A. Susner, M. Majoros, M. D. Sumption, X. Peng, M. Rindfleisch, M. J. Tomsic, and E. W. Collings, *Supercond. Sci. Technol.* **23**, 045018 (2010).
- <sup>33</sup>X. Xu, S. X. Dou, X. L. Wang, J. H. Kim, J. A. Stride, M. Choucair, W. K. Yeoh, R. K. Zheng, and S. P. Ringer, *Supercond. Sci. Technol.* **23**, 085003 (2010).
- <sup>34</sup>L. Embon, Y. Anahory, A. Suhov, D. Halbertal, J. Cuppens, A. Yakovenko, A. Uri, Y. Myasoedov, M. L. Rappaport, M. E. Huber, A. Gurevich, and E. Zeldov, *Sci. Rep.* **5**, 7598 (2015).